An introduction to Hybrid High-Order methods

Daniele A. Di Pietro

Institut Montpelliérain Alexander Grothendieck

New Trends in Compatible Discretizations, 29-30 June 2015

μBibliography: Lowest-order polyhedral methods

- Mimetic Finite Differences
  - Application to polyhedral meshes [Kuznetsov et al., 2004]
  - Convergence analysis [Brezzi et al., 2005]
- Mixed/Hybrid Finite Volumes
  - Pure diffusion (mixed) [Droniou and Eymard, 2006]
  - Pure diffusion (primal) [Eymard et al., 2010]
  - Link with MFD [Droniou et al., 2010]
- More recently
  - Cell-centered Galerkin [DP, 2012]
  - Compatible Discrete Operators [Bonelle and Ern, 2014]
  - Generalized Crouzeix–Raviart [DP and Lemaire, 2015]

μBibliography: High-order polyhedral methods

- Discontinuous Galerkin
  - Unified analysis [Arnold, Brezzi, Cockburn and Marini, 2002]
  - General meshes [DP and Ern, 2010–2012]
  - Adaptive coarsening [Bassi et al., 2012, Antonietti et al., 2013]
- Hybridizable Discontinuous Galerkin
  - Pure diffusion [Cockburn et al., 2009]
- Weak Galerkin
  - Second-order elliptic problems [Wang and Ye, 2013]
- Virtual elements
  - Pure diffusion [Beirão da Veiga et al., 2013a]
  - Nonconforming VEM [Ayuso de Dios et al., 2014]
- Hybrid High-Order (HHO)
  - Pure diffusion [DP and Ern, 2014b]
  - Locally degenerate transport [DP, Droniou and Ern, 2015]

Features of HHO

- Capability of handling general polyhedral meshes
- Construction valid for arbitrary space dimensions
- Arbitrary approximation order (including $k = 0$)
- Physical fidelity
  - Local conservation
  - Locking-free elasticity
  - Péclet-robust transport
  - Stokes flow driven by large irrotational forces
- Reduced computational cost after hybridization

$$N_{\mathrm{dof}}^{\mathrm{hho}} \approx \frac{1}{2} k^2 \,\mathrm{card}(\mathcal{F}_h) \qquad N_{\mathrm{dof}}^{\mathrm{dg}} \approx \frac{1}{6} k^3 \,\mathrm{card}(\mathcal{T}_h)$$

Outline

Outline

Mesh regularity I

Definition (Mesh regularity)

We consider a sequence $(\mathcal{T}_h)_{h \in \mathcal{H}}$ of polyhedral meshes s.t., for all $h \in \mathcal{H}$, $\mathcal{T}_h$ admits a simplicial submesh $\mathfrak{T}_h$ and $(\mathfrak{T}_h)_{h \in \mathcal{H}}$ is

- shape-regular in the usual sense of Ciarlet;
- contact-regular, i.e., every simplex $S \subset T$ is s.t. $h_S \approx h_T$.

Main consequences:

- Trace and inverse inequalities
- Optimal approximation for broken polynomial spaces

Mesh regularity II

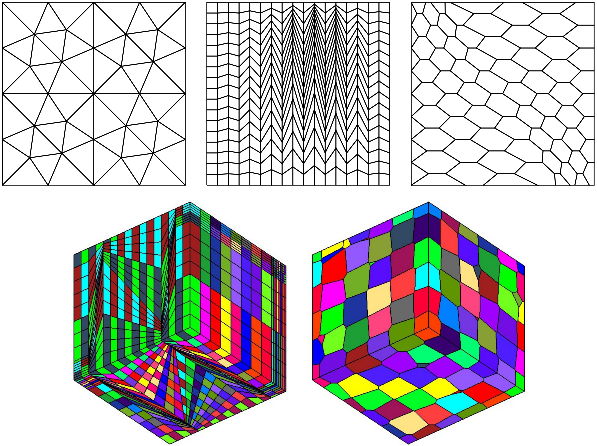

Figure: Admissible meshes in 2d and 3d: [Herbin and Hubert, 2008, FVCA5] and [Di Pietro and Lemaire, 2015] (above) and [Eymard et al., 2011, FVCA6] (below)

Model problem

- Let Ω denote a bounded, connected polyhedral domain
- For $f \in L^2(\Omega)$, we consider the Poisson problem

$$\begin{aligned} -\triangle u &= f \qquad \text{in } \Omega \\ u &= 0 \qquad \text{on } \partial\Omega \end{aligned}$$

- In weak form: Find $u \in H_0^1(\Omega)$ s.t.

$$a(u,v) := (\nabla u, \nabla v) = (f,v) \qquad \forall v \in H_0^1(\Omega)$$

Key ideas

- DOFs: polynomials of degree $k \geqslant 0$ at elements and faces
- Differential operators reconstructions taylored to the problem:

$$\boxed{a_{|T}(u,v) \approx (\boldsymbol{\nabla} p_T^{k+1}\underline{u}_T, \boldsymbol{\nabla} p_T^{k+1}\underline{v}_T) + \text{stab.}}$$

  with
  - high-order reconstruction p_T^{k+1} from local Neumann solves
  - stabilization via face-based penalty
- Construction yielding supercloseness on general meshes

DOFs

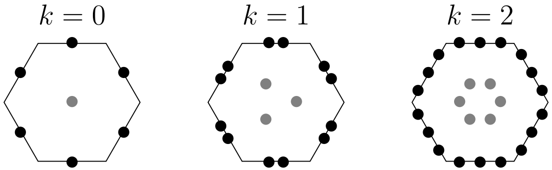

Figure: $\underline{U}_T^k$ for $k \in \{0, 1, 2\}$

- For $k \geqslant 0$ and all $T \in \mathcal{T}_h$, we define the local space of DOFs

$$\underline{U}_T^k := \mathbb{P}_d^k(T) \times \left\{ \bigtimes_{F \in \mathcal{F}_T} \mathbb{P}_{d-1}^k(F) \right\}$$

- The global space has single-valued interface DOFs

$$\underline{U}_h^k := \left\{ \bigtimes_{T \in \mathcal{T}_h} \mathbb{P}_d^k(T) \right\} \times \left\{ \bigtimes_{F \in \mathcal{F}_h} \mathbb{P}_{d-1}^k(F) \right\}$$

Local potential reconstruction I

- Let $T \in \mathcal{T}_h$. The local potential reconstruction operator

$$p_T^{k+1} : \underline{U}_T^k \to \mathbb{P}_d^{k+1}(T)$$

is s.t. $\forall \underline{v}_T \in \underline{U}_T^k$, $(p_T^{k+1}\underline{v}_T, 1)_T = (v_T, 1)_T$ and $\forall w \in \mathbb{P}_d^{k+1}(T)$,

$$\boxed{(\boldsymbol{\nabla} p_T^{k+1}\underline{v}_T, \boldsymbol{\nabla} w)_T := -(v_T, \triangle w)_T + \sum_{F \in \mathcal{F}_T} (v_F, \boldsymbol{\nabla} w \cdot \boldsymbol{n}_{TF})_F}$$

- To compute p_T^{k+1}, we invert a small SPD matrix of size

$$N_{k,d} := \binom{k+1+d}{k+1}$$

- **Trivially parallel task, perfectly suited to GPUs!**

Local potential reconstruction II

Lemma (Approximation properties for $p_T^{k+1}\underline{I}_T^k$)

Define the local reduction map $\underline{I}_T^k : H^1(T) \to \underline{U}_T^k$ *s.t.*

$$\underline{I}_T^k : v \mapsto \left(\pi_T^k v, (\pi_F^k v)_{F \in \mathcal{F}_T}\right).$$

Then, for all $T \in \mathcal{T}_h$ *and all* $v \in H^{k+2}(T)$,

$$\|v - p_T^{k+1}\underline{I}_T^k v\|_T + h_T \|\boldsymbol{\nabla}(v - p_T^{k+1}\underline{I}_T^k v)\|_T \lesssim h_T^{k+2}\|v\|_{k+2,T}.$$

Local potential reconstruction III

- Since $\triangle w \in \mathbb{P}_d^{k-1}(T)$ and $\nabla w_{|F}\cdot \boldsymbol{n}_{TF} \in \mathbb{P}_{d-1}^k(F)$,

$$
\begin{aligned}
(\nabla p_T^{k+1} \underline{I}_T^k v, \nabla w)_T &= -(\pi_T^k v, \triangle w)_T + \sum_{F\in\mathcal{F}_T} (\pi_F^k v, \nabla w\cdot \boldsymbol{n}_{TF})_F \\
&= -(v, \triangle w)_T + \sum_{F\in\mathcal{F}_T} (v, \nabla w\cdot \boldsymbol{n}_{TF})_F \\
&= (\nabla v, \nabla w)_T
\end{aligned}
$$

- This shows that $p_T^{k+1}\underline{I}_T^k$ is the elliptic projector on $\mathbb{P}_d^{k+1}(T)$:

$$
(\nabla p_T^{k+1} \underline{I}_T^k v - \nabla v, \nabla w)_T = 0 \qquad \forall w \in \mathbb{P}_d^{k+1}(T)
$$

- The approximation properties follow

Stabilization I

- The following local discrete bilinear form is in general not stable

$$a_T(\underline{u}_T, \underline{v}_T) = (\nabla p_T^{k+1}\underline{u}_T, \nabla p_T^{k+1}\underline{v}_T)_T$$

- As a remedy, we add a local stabilization term:

$$\boxed{a_T(\underline{u}_T, \underline{v}_T) := (\nabla p_T^{k+1}\underline{u}_T, \nabla p_T^{k+1}\underline{v}_T)_T + s_T(\underline{u}_T, \underline{v}_T)}$$

- We aim at expressing coercivity w.r.t. to the local (semi-)norm

$$\|\underline{v}_T\|_{1,T}^2 := \|\nabla v_T\|_T^2 + \sum_{F\in\mathcal{F}_T} \frac{1}{h_F}\|v_F - v_T\|_F^2$$

Stabilization II

- A naive choice for the stabilization would be (cf. HDG)

$$s_T(\underline{u}_T, \underline{v}_T) := \sum_{F\in\mathcal{F}_T} \frac{1}{h_F}(u_F - u_T, v_F - v_T)_F$$

- This choice, however, is suboptimal since, for all $v \in H^{k+2}(T)$,

$$\|\boldsymbol{\nabla}(p_T^{k+1}\underline{I}_T^k v - v)\|_T \lesssim h^{k+1}\|v\|_{H^{k+2}(T)},$$
$$s_T(\underline{I}_T^k v, \underline{I}_T^k v)^{1/2} \lesssim h^{k}\|v\|_{H^{k+1}(T)}$$

- **We need to penalize higher-order differences!**

Stabilization III

- Let us introduce the face residual operator $r_{TF}^k : \underline{U}_T^k \to \mathbb{P}_{d-1}^k(F)$ s.t.

$$r_{TF}^k(\underline{v}_T) := \pi_F^k(v_F - p_T^{k+1}\underline{v}_T) - \pi_T^k(v_T - p_T^{k+1}\underline{v}_T)$$

- Consider the following least-square penalty bilinear form:

$$\boxed{s_T(\underline{u}_T, \underline{v}_T) := \sum_{F \in \mathcal{F}_T} \frac{1}{h_F}(r_{TF}^k \underline{u}_T, r_{TF}^k \underline{v}_T)_F}$$

- With this choice, it can be proved that, for all $\underline{v}_T \in \underline{U}_T^k$,

$$\|\underline{v}_T\|_{1,T}^2 \lesssim a_T(\underline{v}_T, \underline{v}_T) \lesssim \|\underline{v}_T\|_{1,T}^2$$

Stabilization IV

- Let us investigate the consistency properties of s_T
- Using approximation for $p_T^{k+1}\underline{I}_T^k$ we have, for all $v \in H^{k+2}(T)$,

$$\begin{aligned}
\|r_{TF}^k \underline{I}_T^k v\|_F &= \|\pi_F^k(v - p_T^{k+1}\underline{I}_T^k v) - \pi_T^k(v - p_T^{k+1}\underline{I}_T^k v)\|_F \\
&\leqslant \|\pi_F^k(v - p_T^{k+1}\underline{I}_T^k v)\|_F + \|\pi_T^k(v - p_T^{k+1}\underline{I}_T^k v)\|_F \\
&\lesssim \|v - p_T^{k+1}\underline{I}_T^k v\|_F + h_T^{-1/2}\|v - p_T^{k+1}\underline{I}_T^k v\|_T \\
&\lesssim h_T^{k+3/2}\|v\|_{H^{k+2}(T)}
\end{aligned}$$

- Hence, this time

$$\boxed{s_T(\underline{I}_T^k v, \underline{I}_T^k v)^{1/2} \lesssim h_T^{k+1}\|v\|_{H^{k+2}(T)}}$$

Stabilization V

- Alternative interpretation: Define $\widehat{p}_T^{k+1} : \underline{U}_T^k \to \mathbb{P}_d^{k+1}(T)$ s.t.

$$\widehat{p}_T^{k+1}\underline{v}_T := v_T + (p_T^{k+1}\underline{v}_T - \pi_T^k p_T^{k+1}\underline{v}_T)$$

- $\widehat{p}_T^{k+1}\underline{v}_T$ is a high-order correction of cell DOFs
- It can be proved that s_T admits the equivalent formulation

$$\boxed{s_T(\underline{u}_T, \underline{v}_T) := \sum_{F\in\mathcal{F}_T} \frac{1}{h_F}(\pi_F^k(\widehat{p}_T^{k+1}\underline{u}_T - u_F), \pi_F^k(\widehat{p}_T^{k+1}\underline{v}_T - v_F))_F}$$

Discrete problem

- We enforce boundary conditions strongly considering the space

$$\underline{U}_{h,0}^k := \left\{ \underline{v}_h \in \underline{U}_h^k \mid v_F \equiv 0 \quad \forall F \in \mathcal{F}_h^{\mathrm{b}} \right\}$$

- The discrete problem reads: Find $\underline{u}_h \in \underline{U}_{h,0}^k$ s.t.

$$\boxed{a_h(\underline{u}_h, \underline{v}_h) := \sum_{T \in \mathcal{T}_h} a_T(\underline{u}_T, \underline{v}_T) = \sum_{T \in \mathcal{T}_h} (f, v_T)_T \qquad \forall \underline{v}_h \in \underline{U}_{h,0}^k}$$

- Well-posedness follows from the $\|\cdot\|_{1,h}$-coercivity of a_h with

$$\|\underline{v}_h\|_{1,h}^2 := \sum_{T \in \mathcal{T}_h} \|\underline{v}_T\|_{1,T}^2$$

Convergence I

Theorem (Energy-norm error estimate)

Assume $u \in H^{k+2}(\Omega)$ *and define the global reduction map*

$$\underline{I}_h^k u := \big((\pi_T^k u)_{T\in\mathcal{T}_h}, (\pi_F^k u)_{F\in\mathcal{F}_h}\big) \in \underline{U}_{h,0}^k.$$

Then, we have the following energy error estimate:

$$\boxed{\|\underline{u}_h - \underline{I}_h^k u\|_{1,h} \lesssim h^{k+1}\|u\|_{H^{k+2}(\Omega)}.}$$

Convergence II

Theorem (L^2-norm error estimate)

Further assuming *elliptic regularity* *and* $f \in H^1(\Omega)$ *if* $k = 0$,

$$\boxed{\|u_h - \pi_h^k u\| \lesssim h^{k+2} B(u,k),}$$

with $B(u,0) := \|f\|_{H^1(\Omega)}$, $B(u,k) := \|u\|_{H^{k+2}(\Omega)}$ *if* $k \geqslant 1$ *and*

$$u_{h|T} = u_T \qquad \forall T \in \mathcal{T}_h.$$

Corollary (L^2-norm estimate for $p_T^{k+1}\underline{u}_T$)

The reconstruction $p_T^{k+1}\underline{u}_T$ *converges to* u *as* h^{k+2} *in the* L^2*-norm.*

Convergence for a smooth 2d solution I

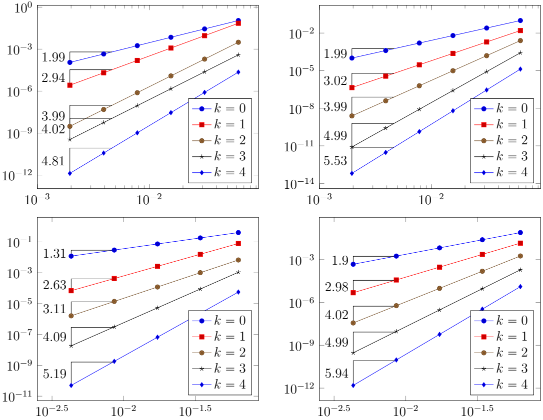

Figure: Energy (left) and L^2-norm (right) of the error vs. h for uniformly refined triangular (top) and hexagonal (bottom) mesh families, $u(\boldsymbol{x}) = \sin(\pi x_1)\sin(\pi x_2)$

Convergence for a smooth 2d solution II

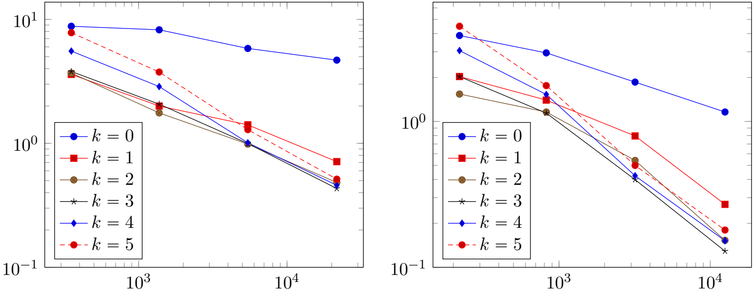

Figure: Assembly/solution time for triangular (left) and hexagonal (right) mesh families, sequential implementation

Mesh adaptivity: Fichera's 3d test case I

- Let $\Omega := (-1,1)^3 \backslash [0,1]^3$
- We consider the following exact solution:

$$u(\boldsymbol{x}) = (x_1^2 + x_2^2 + x_3^2)^{\frac{1}{4}}$$

corresponding to the forcing term

$$f(\boldsymbol{x}) = -\frac{3}{4}(x_1^2 + x_2^2 + x_3^2)^{-\frac{3}{4}}$$

- We consider an a posteriori-driven adaptive procedure

Mesh adaptivity: Fichera's 3d test case II

Theorem (A posteriori error estimate [DP and Specogna, 2015])

It holds with $p_h^{k+1}\underline{u}_h \in \mathbb{P}_d^{k+1}(\mathcal{T}_h)$ *s.t.* $(p_h^{k+1}\underline{u}_h)_{|T} = p_T^{k+1}\underline{u}_T \ \forall T \in \mathcal{T}_h$,

$$\|\nabla(p_h^{k+1}\underline{u}_h - u)\|^2 \leqslant \sum_{T\in\mathcal{T}_h} \left\{\eta_{\mathrm{nc},T}^2 + (\eta_{\mathrm{res},T} + \eta_{\mathrm{sta},T})^2\right\},$$

where, denoting by u_h^* *is the Oswald interpolate of* $p_h^{k+1}\underline{u}_h$,

$$\begin{aligned}
\eta_{\mathrm{nc},T} &:= \|\nabla(p_T^{k+1}\underline{u}_T - u_h^*)\|_T,\\
\eta_{\mathrm{res},T} &:= C_{\mathrm{P},T} h_T \|(f + \triangle p_T^{k+1}\underline{u}_T) - \pi_T^0(f + \triangle p_T^{k+1}\underline{u}_T)\|_T,\\
\eta_{\mathrm{sta},T} &:= C_{\mathrm{F},T} h_T^{1/2} \|R_{\partial T}^{*,k}(\tau_{\partial T} R_{\partial T}^k(u_T - u_{\partial T}))\|_{\partial T},
\end{aligned}$$

with $R_{\partial T}^k$, $R_{\partial T}^{*,k}$ *and* $\tau_{\partial T}$ *defined as for flux the formulation (cf. below).*

Mesh adaptivity: Fichera's 3d test case III

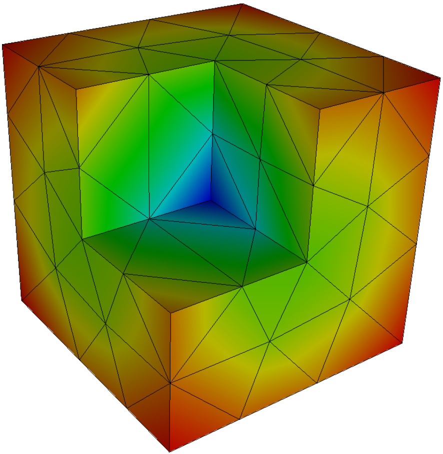

Figure: HHO solution on a sequence of adaptively refined simplicial meshes

Mesh adaptivity: Fichera's 3d test case IV

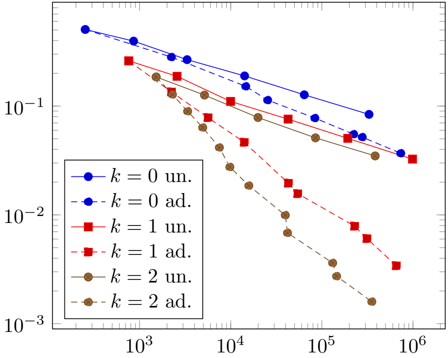

Figure: Energy error vs. $\dim(\underline{U}_h^k)$

Mesh adaptivity: Fichera's 3d test case V

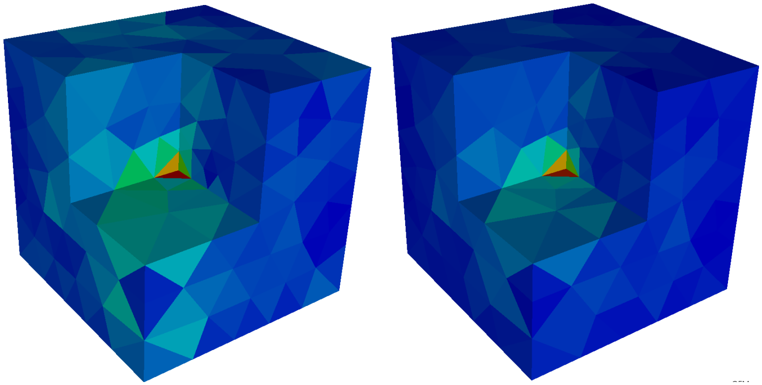

Figure: Estimated (left) and true (right) error distribution

Outline

Variable diffusion I

- Let $\boldsymbol{\nu} : \Omega \to \mathbb{R}^{d\times d}$ be a SPD tensor-valued field s.t.

$$\forall T \in \mathcal{T}_h, \qquad 0 < \underline{\nu}_T \leqslant \lambda(\boldsymbol{\nu}) \leqslant \overline{\nu}_T$$

- For the sake of simplicity, we assume $\boldsymbol{\nu}$ polynomial on $\mathcal{T}_h$,

$$\exists l \in \mathbb{N}^*, \qquad \boldsymbol{\nu} \in \mathbb{P}_d^l(\mathcal{T}_h)^{d\times d}$$

- We consider the Darcy problem

$$\begin{aligned} -\boldsymbol{\nabla}\cdot(\boldsymbol{\nu}\boldsymbol{\nabla} u) &= f \qquad \text{in } \Omega \\ u &= 0 \qquad \text{on } \partial\Omega \end{aligned}$$

Variable diffusion II

$$\boxed{(\boldsymbol{\nu}\boldsymbol{\nabla}p_T^{k+1}\underline{v}_T, \boldsymbol{\nabla}w)_T = (\boldsymbol{\nu}\boldsymbol{\nabla}v_T, \boldsymbol{\nabla}w)_T + \sum_{F\in\mathcal{F}_T}(v_F - v_T, \boldsymbol{\nu}\boldsymbol{\nabla}w\cdot\boldsymbol{n}_{TF})_F}$$

Lemma (Approximation properties of $p_T^{k+1}\underline{I}_T^k$)

For all $v \in H^{k+2}(T)$, with $\alpha = \frac{1}{2}$ if $l = 0$ and $\alpha = 1$ if $l \geqslant 1$,

$$\|v - p_T^{k+1}\underline{I}_T^k v\|_T + h_T\|\boldsymbol{\nabla}(v - p_T^{k+1}\underline{I}_T^k v)\|_T \leqslant C\rho_T^{\alpha}h_T^{k+2}\|v\|_{k+2,T},$$

with local heterogeneity/anisotropy ratio $\rho_T := \frac{\overline{\nu}_T}{\underline{\nu}_T} \geqslant 1$.

Variable diffusion III

Theorem (Energy-error estimate)

Assume that $u \in H^{k+2}(\mathcal{T}_h)$ *and set*

$$a_{\boldsymbol{\nu},T}(\underline{u}_T, \underline{v}_T) := (\boldsymbol{\nu}\boldsymbol{\nabla} p_T^{k+1}\underline{u}_T, \boldsymbol{\nabla} p_T^{k+1}\underline{v}_T)_T + s_{\boldsymbol{\nu},T}(\underline{u}_T, \underline{v}_T)$$

where, letting $\nu_{TF} := \|\boldsymbol{n}_{TF}\cdot\boldsymbol{\nu}_{|T}\cdot\boldsymbol{n}_{TF}\|_{L^\infty(F)}$,

$$s_{\boldsymbol{\nu},T}(\underline{u}_T, \underline{v}_T) := \sum_{F\in\mathcal{F}_T} \frac{\nu_{TF}}{h_F}(\pi_F^k(\widehat{p}_T^{k+1}\underline{u}_T - u_F), \pi_F^k(\widehat{p}_T^{k+1}\underline{v}_T - v_F))_F.$$

Then, with α *as above and* $\|\cdot\|_{\boldsymbol{\nu},h}$ *denoting the norm defined by* $a_{\boldsymbol{\nu},h}$,

$$\boxed{\|\underline{u}_h - \underline{I}_h^k u\|_{\boldsymbol{\nu},h} \lesssim \left\{\sum_{T\in\mathcal{T}_h} \overline{\nu}_T \rho_T^{1+2\alpha} h_T^{2(k+1)} \|u\|_{k+2,T}^2\right\}^{1/2}.}$$

Le Potier's test case I

- We consider the smooth exact solution

$$u(\boldsymbol{x}) = \sin(\pi x_1)\sin(\pi x_2),$$

- The diffusion field has rotating principal axes

$$\boldsymbol{\nu}(\boldsymbol{x}) = \begin{pmatrix} (x_2 - \overline{x}_2)^2 + \epsilon(x_1 - \overline{x}_1)^2 & -(1-\epsilon)(x_1 - \overline{x}_1)(x_2 - \overline{x}_2) \\ -(1-\epsilon)(x_1 - \overline{x}_1)(x_2 - \overline{x}_2) & (x_1 - \overline{x}_1)^2 + \epsilon(x_2 - \overline{x}_2)^2 \end{pmatrix},$$

with anisotropy ratio and rotation center

$$\epsilon = \rho^{-1} = 1 \cdot 10^{-2}, \qquad (\overline{x}_1, \overline{x}_2) = -(0.1, 0.1)$$

Le Potier's test case II

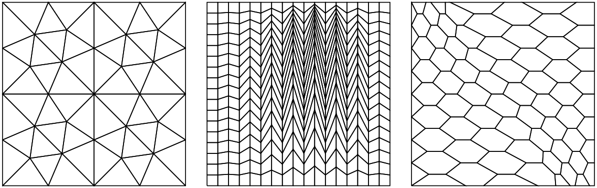

Figure: Triangular, Kershaw and hexagonal mesh families

Le Potier's test case III

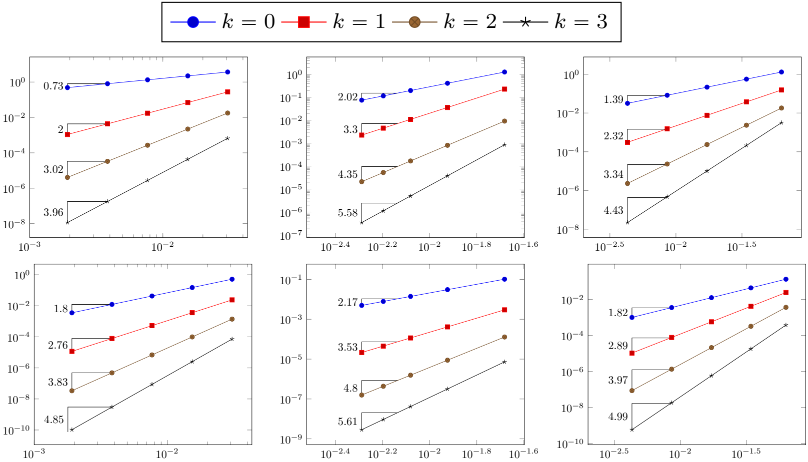

Figure: $\|\cdot\|_{1,h}$-norm (above) and L^2-norm (below) of the error vs. h for the triangular, Kershaw and hexagonal mesh families

Local conservation and numerical fluxes I

- A highly prized property in practice is local conservation
- At the discrete level, we wish to mimick the local balance

$$(\boldsymbol{\nu}_T \boldsymbol{\nabla} u, \boldsymbol{\nabla} v)_T - \sum_{F \in \mathcal{F}_T} (\boldsymbol{\nu}_T \boldsymbol{\nabla} u \cdot \boldsymbol{n}_{TF}, v)_F = (f, v)_T \quad \forall v \in H^1(T)$$

where, for every interface $F \in \mathcal{F}_{T_1} \cap \mathcal{F}_{T_2}$,

$$\boldsymbol{\nu}_{T_1} \boldsymbol{\nabla} u \cdot \boldsymbol{n}_{T_1 F} + \boldsymbol{\nu}_{T_2} \boldsymbol{\nabla} u \cdot \boldsymbol{n}_{T_2 F} = 0$$

- This requires to identify numerical fluxes

Local conservation and numerical fluxes II

- Define the boundary residual operator $R^k_{\partial T} : \mathbb{P}^k_{d-1}(\mathcal{F}_T) \to \mathbb{P}^k_{d-1}(\mathcal{F}_T)$

$$R^k_{\partial T}\varphi_{|F} := \pi^k_F \left(\varphi_{|F} - p^{k+1}_T(0,\varphi) + \pi^k_T p^{k+1}_T(0,\varphi)\right) \quad \forall F \in \mathcal{F}_T$$

- Denote by $R^{*,k}_{\partial T}$ its adjoint and let $\tau_{\partial T}$ and $u_{\partial T}$ be s.t.

$$\tau_{\partial T|F} = \frac{\nu_{TF}}{h_F} \quad \text{and} \quad u_{\partial T|F} = u_F \quad \forall F \in \mathcal{F}_T$$

- Then, the penalty term can be rewritten in conservative form as

$$\boxed{s_T(\underline{u}_T, \underline{v}_T) = \sum_{F\in\mathcal{F}_T} \left(R^{*,k}_{\partial T}(\tau_{\partial T} R^k_{\partial T}(u_{\partial T} - u_T)), v_F - v_T\right)_F}$$

Local conservation and numerical fluxes III

Lemma (Flux formulation)

The HHO solution $\underline{u}_h \in \underline{U}_{h,0}^k$ *satisfies, for all* $T \in \mathcal{T}_h$ *and all* $v_T \in \mathbb{P}_d^k(T)$

$$(\boldsymbol{\nu}\boldsymbol{\nabla} p_T^{k+1}\underline{u}_T, \boldsymbol{\nabla} v_T)_T - \sum_{F\in\mathcal{F}_T} (\Phi_{TF}(\underline{u}_T), v_T)_F = (f, v_T)_T,$$

with numerical flux

$$\Phi_{TF}(\underline{u}_T) := \boldsymbol{\nu}_T \boldsymbol{\nabla} p_T^{k+1}\underline{u}_T \cdot \boldsymbol{n}_{TF} - R_{\partial T}^{*,k}(\tau_{\partial T} R_{\partial T}^k(u_{\partial T} - u_T)),$$

s.t., for every interface $F \in \mathcal{F}_{T_1} \cap \mathcal{F}_{T_2}$*,*

$$\Phi_{T_1F}(\underline{u}_{T_1}) + \Phi_{T_2F}(\underline{u}_{T_2}) = 0.$$

Link with HDG

- The flux formulation shows that (cf. [Cockburn, DP and Ern, 2015])

$$\text{HHO} = \text{HDG on steroids}$$

- Smaller local problems to eliminate flux unknowns:

$$\boldsymbol{\nabla}\mathbb{P}_d^{k+1}(T) \quad \text{vs.} \quad \mathbb{P}_d^k(T)^d$$

- Superconvergence of the potential in the L^2-norm

$$h^{k+2} \quad \text{vs.} \quad h^{k+1}$$

- **HHO can be adapted into existing HDG codes!**

The HHO(l) family

- Let $T \in \mathcal{T}_h$, $k-1 \leqslant l \leqslant k+1$, and consider the local space

$$\underline{U}_T^{k,l} := \mathbb{P}_d^l(T) \times \left\{ \bigtimes_{F \in \mathcal{F}_T} \mathbb{P}_{d-1}^k(F) \right\}$$

- Convergence rates as for the original HHO method and
  - $l = k-1$: High-Order Mimetic (up to variants in stabilization)
  - $l = k$: original HHO method
  - $l = k+1$: new HDG method
- $k = 0$ and $l = k-1$ on simplices yields the Crouzeix–Raviart element
- **The globally-coupled unknowns coincide in all the cases!**

A nonconforming finite element interpretation I

- We interpret the HHO(l) methods as nonconforming FE methods
- The construction extends the ideas of [Ayuso de Dios et al., 2014]
- For the conforming case, cf. F. Brezzi's talk
- For a fixed element $T \in \mathcal{T}_h$, we define the local space

$$\boxed{V_T^{k,l} := \left\{\varphi \in H^1(T) \mid \ \nabla\varphi_{|F}\cdot\boldsymbol{n}_F \in \mathbb{P}_{d-1}^k(F)\ \forall F \in \mathcal{F}_T \text{ and } \triangle\varphi \in \mathbb{P}_d^l(T)\ \right\}}$$

- We next study the relation between $V_T^{k,l}$ and $\underline{U}_T^{k,l}$

A nonconforming finite element interpretation II

- Let $\Phi_T : \underline{U}_T^{k,l} \to V_T^{k,l}$ be s.t. $\Phi_T(\underline{v}_T)$ solves the Neumann problem

$$\boxed{\triangle \Phi_T(\underline{v}_T) = v_T - \frac{1}{|T|_d}\left(\int_T v_T - \sum_{F\in\mathcal{F}_T}\int_F v_F\right)}$$

and

$$\boldsymbol{\nabla}\Phi_T(\underline{v}_T)_{|F}\cdot\boldsymbol{n}_{TF} = v_F \quad \forall F\in\mathcal{F}_T, \qquad \int_T \Phi_T(\underline{v}_T) = \int_T v_T$$

- Clearly, both Φ_T and $\underline{I}_T^{k,l} : V_T^{k,l} \to \underline{U}_T^{k,l}$ are injective
- Therefore, $\underline{I}_T^{k,l} : V_T^{k,l} \to \underline{U}_T^{k,l}$ is an isomorphism and we can identify

$$\boxed{V_T^{k,l} \sim \underline{U}_T^{k,l}}$$

A nonconforming finite element interpretation III

- $\underline{U}_T^k$ contains the DOFs for $V_T^{k,l}$ as defined by $\underline{I}_T^k$
- Functions in $V_T^{k,l}$ are not directly available, but DOFs in $\underline{U}_T^k$ are
- We define the computable projection $\Pi_T^{k+1} : V_T^{k,l} \to \mathbb{P}_d^{k+1}(T)$ s.t.

$$\boxed{\Pi_T^{k+1}\varphi := p_T^{k+1}\underline{I}_T^{k,l}\varphi}$$

- Moreover, for all $\varphi \in V_T^{k,l}$, the face residual rewrites

$$\boxed{r_{TF}^k \underline{I}_T^k \varphi = \pi_F^k(\Pi_T^{k+1}\varphi - \varphi) - \pi_T^k(\Pi_T^{k+1}\varphi - \varphi)}$$

The case $l = k + 1$

- Some simplifications hold for the case $k = l + 1$
- As a matter of fact, one has

$$\widehat{p}_T^{k,l} \underline{v}_T = v_T + (p_T^{k+1} \underline{v}_T - \pi_T^{k+1} p_T^{k+1} \underline{v}_T) = v_T$$

- Hence, the stabilization bilinear form s_T simply rewrites

$$s_T^{\mathrm{hdg}}(\underline{u}_T, \underline{v}_T) := \sum_{F \in \mathcal{F}_T} \frac{1}{h_F} (\pi_F^k(u_T - u_F), \pi_F^k(v_T - v_F))_F$$

- This corresponds to a new HDG-like method

Outline

Yesterday's course in a nutshell

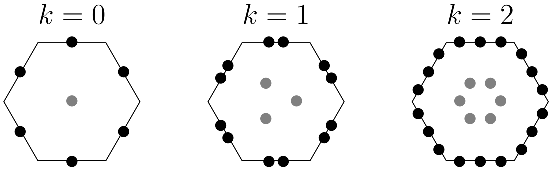

Figure: $\underline{U}_T^k$ for $k \in \{0, 1, 2\}$

- High-order potential reconstruction p_T^{k+1} from Neumann solves
- High-order face-based stabilisation bilinear form s_T
- Global problem from the assembly of local bilinear forms

$$\boxed{a_T(\underline{u}_T, \underline{v}_T) = (\nabla p_T^{k+1} \underline{u}_T, \nabla p_T^{k+1} \underline{v}_T) + s_T(\underline{u}_T, \underline{v}_T)}$$

- Construction yielding supercloseness on general meshes

Continuous setting I

- Consider the 1d problem, cf. [Gastaldi and Quarteroni, 1989]:

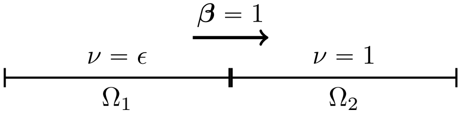

- As $\epsilon \to 0^+$, a boundary layer develops at $x = 1/2$
- When $\epsilon = 0$, it turns into a jump discontinuity

Continuous setting II

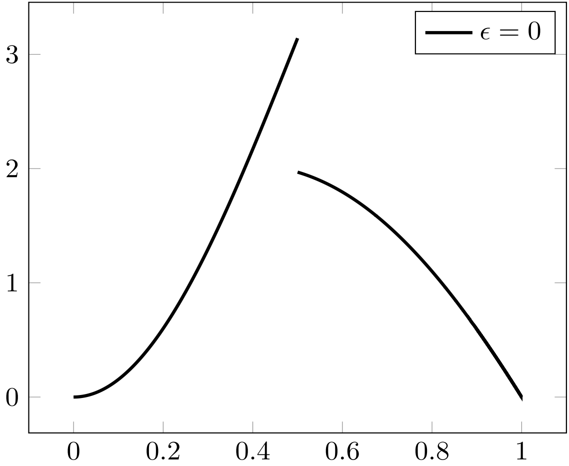

Figure: Solutions for different values of ϵ

Continuous setting III

- Let us now consider $d \geqslant 1$ with diffusion coefficient $\nu : \Omega \to \mathbb{R}^+$
- Let $P_\Omega := \{\Omega_i\}$ denote a polyhedral partition of Ω
- We assume $\nu \in \mathbb{P}^0_d(P_\Omega)$ and s.t.

$$\nu \geqslant \underline{\nu} \geqslant 0 \text{ a.e. in } \Omega$$

- **ν can vanish in some subdomain Ω_i!**
- Full diffusion tensors could also be considered

Continuous setting IV

- We assume that both advection and reaction are present
- The advective velocity $\boldsymbol{\beta} : \Omega \to \mathbb{R}^d$ is assumed s.t.

$$\boldsymbol{\beta} \in \mathrm{Lip}(\Omega)^d$$

- For the sake of simplicity, we also take $\boldsymbol{\beta}$ incompressible,

$$\boldsymbol{\nabla} \cdot \boldsymbol{\beta} \equiv 0$$

- For the reaction coefficient $\mu : \Omega \to \mathbb{R}$, we assume

$$\mu \in L^\infty(\Omega) \text{ and } \mu \geqslant \mu_0 > 0 \text{ a.e. in } \Omega$$

Continuous setting V

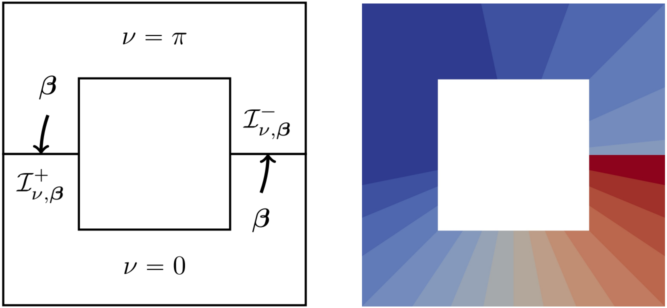

Figure: Two-dimensional example from [DP, Ern and Guermond, 2008]

Continuous setting VI

- We define $\mathcal{I}_\nu$ as the set of points in Ω in $\partial\Omega_i \cap \partial\Omega_j$ s.t.

$$\nu_{|\Omega_i} > \nu_{|\Omega_j} = 0$$

- Boundary conditions can only be enforced on

$$\Gamma_{\nu,\boldsymbol{\beta}} := \{\boldsymbol{x} \in \partial\Omega \mid \nu > 0 \text{ or } \boldsymbol{\beta}\cdot\boldsymbol{n} < 0\}$$

- For well-posedness, transmission conditions are required on

$$\mathcal{I}^{\pm}_{\nu,\boldsymbol{\beta}} := \{\boldsymbol{x} \in \mathcal{I}_\nu \mid \pm(\boldsymbol{\beta}\cdot\boldsymbol{n}_{\Omega_i})(\boldsymbol{x}) > 0\}$$

Continuous setting VII

- Let $f \in L^2(\Omega)$ and $g \in L^2(\Gamma_{\nu,\boldsymbol{\beta}})$. We seek $u : \Omega \to \mathbb{R}$ s.t.

$$\begin{aligned} \boldsymbol{\nabla}\cdot(-\nu\boldsymbol{\nabla}u + \boldsymbol{\beta}u) + \mu u = f &\quad \text{in } \Omega\backslash\mathcal{I}_\nu, \\ u = g &\quad \text{on } \Gamma_{\nu,\boldsymbol{\beta}} \end{aligned}$$

- The transmission conditions that warrant well-posedness are

$$\begin{aligned} [-\nu\boldsymbol{\nabla}u + \boldsymbol{\beta}u]\cdot\boldsymbol{n}_{\Omega_i} = 0 &\quad \text{on } \mathcal{I}_\nu, \\ [u] = 0 &\quad \text{on } \mathcal{I}^+_{\nu,\boldsymbol{\beta}} \end{aligned}$$

- **The solution u can jump across $\mathcal{I}^-_{\nu,\boldsymbol{\beta}}$!**
- For a weak formulation, cf. [DP, Ern and Guermond, 2008]

Key ideas

- Discrete advective derivative satisfying a discrete IBP formula
- Upwind stabilization using cell and face unknowns
  - Independent control for the advective part
  - Consistency also on $\mathcal{I}^{-}_{\nu,\boldsymbol{\beta}}$, where u jumps
- Weakly enforced boundary conditions
  - Extension of Nitsche's ideas to HHO
  - Automatic detection of $\Gamma_{\nu,\boldsymbol{\beta}}$

Features

- Polyhedral meshes and arbitrary approximation order $k \geqslant 0$
- Method valid for the full range of local Peclet numbers
- Analysis capturing the variation in the convergence rate
- **No need to duplicate interface unknowns on $\mathcal{I}^-_{\nu,\boldsymbol{\beta}}$ (!)**

Advective derivative I

- The discrete advective derivative

$$G^k_{\boldsymbol{\beta},T} : \underline{U}^k_T \to \mathbb{P}^k_d(T)$$

is s.t., for all $\underline{v}_T \in \underline{U}^k_T$ and all $w \in \mathbb{P}^k_d(T)$,

$$\boxed{(G^k_{\boldsymbol{\beta},T}\underline{v}_T, w)_T = -(v_T, \boldsymbol{\beta}\cdot\boldsymbol{\nabla} w)_T + \sum_{F\in\mathcal{F}_T} ((\boldsymbol{\beta}\cdot\boldsymbol{n}_{TF})v_F, w)_F}$$

- For stability, we need a discrete IBP formula mimicking

$$(\boldsymbol{\beta}\cdot\boldsymbol{\nabla} w, v)_\Omega + (w, \boldsymbol{\beta}\cdot\boldsymbol{\nabla} v)_\Omega = ((\boldsymbol{\beta}\cdot\boldsymbol{n})w, v)_{\partial\Omega}$$

Advective derivative II

Lemma (Discrete IBP formula)

For all $\underline{w}_h, \underline{v}_h \in \underline{U}_h^k$ *it holds*

$$\sum_{T\in\mathcal{T}_h} \left\{ (G_{\boldsymbol{\beta},T}^k \underline{w}_T, v_T)_T + (w_T, G_{\boldsymbol{\beta},T}^k \underline{v}_T)_T \right\} = \sum_{F\in\mathcal{F}_h^{\mathrm{b}}} ((\boldsymbol{\beta}\cdot\boldsymbol{n}_F) w_F, v_F)_F - \sum_{T\in\mathcal{T}_h} \sum_{F\in\mathcal{F}_h} ((\boldsymbol{\beta}\cdot\boldsymbol{n}_{TF})(w_F - w_T), v_F - v_T)_F.$$

To control the term in red, we use element-face upwinding

Advection-reaction I

- For all $T \in \mathcal{T}_h$, we let

$$a_{\boldsymbol{\beta},\mu,T}(\underline{w}_T, \underline{v}_T) := -(w_T, G^k_{\boldsymbol{\beta},T}\underline{v}_T)_T + \mu(w_T, v_T)_T + s^-_{\boldsymbol{\beta},T}(\underline{w}_T, \underline{v}_T)$$

with local upwind stabilization bilinear form s.t.

$$s^-_{\boldsymbol{\beta},T}(\underline{w}_T, \underline{v}_T) := \sum_{F\in\mathcal{F}_T} ((\boldsymbol{\beta}\cdot\boldsymbol{n}_{TF})^-(w_F - w_T), v_F - v_T)_F,$$

- Including weak enforcement of BCs, we let

$$\boxed{a_{\boldsymbol{\beta},\mu,h}(\underline{w}_h, \underline{v}_h) := \sum_{T\in\mathcal{T}_h} a_{\boldsymbol{\beta},\mu,T}(\underline{w}_h, \underline{v}_h) + \sum_{F\in\mathcal{F}_h^{\mathrm{b}}} ((\boldsymbol{\beta}\cdot\boldsymbol{n})^+ w_F, v_F)_F}$$

Advection-reaction II

Lemma (Stability of $a_{\boldsymbol{\beta},\mu,h}$)

Let $\eta := \min_{T\in\mathcal{T}_h}(1, \tau_{\mathrm{ref},T}\mu)$, $\tau_{\mathrm{ref},T} := \{\max(\|\mu\|_{L^\infty(T)}, L_{\boldsymbol{\beta},T})\}^{-1}$. *Then,*

$$\boxed{\forall \underline{v}_h \in \underline{U}_h^k, \qquad \eta\|\underline{v}_h\|_{\boldsymbol{\beta},\mu,h}^2 \leqslant a_{\boldsymbol{\beta},\mu,h}(\underline{v}_h, \underline{v}_h),}$$

with global advection-reaction norm

$$\|\underline{v}_h\|_{\boldsymbol{\beta},\mu,h}^2 := \sum_{T\in\mathcal{T}_h} \|\underline{v}_T\|_{\boldsymbol{\beta},\mu,T}^2 + \frac{1}{2}\sum_{F\in\mathcal{F}_h^{\mathrm{b}}} \||\boldsymbol{\beta}\cdot\boldsymbol{n}_{TF}|^{1/2} v_F\|_F^2,$$

and, for all $T \in \mathcal{T}_h$,

$$\|\underline{v}_T\|_{\boldsymbol{\beta},\mu,T}^2 := \frac{1}{2}\sum_{F\in\mathcal{F}_T} \||\boldsymbol{\beta}\cdot\boldsymbol{n}_{TF}|^{1/2}(v_F - v_T)\|_F^2 + \tau_{\mathrm{ref},T}^{-1}\|v_T\|_T^2.$$

Weakly enforced BCs for diffusion I

- We modify the diffusion bilinear form to weakly enforce BCs
- The new bilinear form $a_{\nu,h}$ reads (after setting $\boldsymbol{\nu} = \nu \boldsymbol{I}_d$),

$$\boxed{a_{\nu,h}(\underline{w}_h, \underline{v}_h) := \sum_{T\in\mathcal{T}_h} a_{\nu,T}(\underline{w}_T, \underline{v}_T) + s_{\partial,\nu,h}(\underline{w}_h, \underline{v}_h)}$$

with, for a user-defined penalty parameter $\varsigma > 0$,

$$s_{\partial,\nu,h}(\underline{w}_h, \underline{v}_h) := \sum_{F\in\mathcal{F}_h^{\mathrm{b}}} \left\{ -(\nu_F \boldsymbol{\nabla} p_T^{k+1} \underline{w}_T \cdot \boldsymbol{n}_{TF}, v_F)_F + \frac{\varsigma \nu_F}{h_F}(w_F, v_F)_F \right\}$$

- Symmetric and skew-symmetric variations could also be devised

Weakly enforced BCs for diffusion II

Lemma (Stability of $a_{\nu,h}$)

Assuming that $\varsigma > C_{\rm tr}^2 N_\partial/4$ *it holds, for all* $\underline{v}_h \in \underline{U}_h^k$,

$$a_{\nu,h}(\underline{v}_h,\underline{v}_h) =: \|\underline{v}_h\|_{\nu,h}^2 \simeq \sum_{T\in\mathcal{T}_h} \nu_T \|\underline{v}_T\|_{1,T}^2 + \sum_{F\in\mathcal{F}_h^{\rm b}} \frac{\nu_F}{h_F}\|v_F\|_F^2.$$

Discrete problem I

- Let, accounting for boundary conditions,

$$l_h(\underline{v}_h) := \sum_{T\in\mathcal{T}_h}(f, v_T)_T + \sum_{F\in\mathcal{F}_h^{\mathrm{b}}}\left\{((\boldsymbol{\beta}\cdot\boldsymbol{n}_{TF})^- g, v_F)_F + \frac{\nu_F\varsigma}{h_F}(g, v_F)_F\right\}$$

- The discrete problem reads: Find $\underline{u}_h \in \underline{U}_h^k$ s.t., $\forall \underline{v}_h \in \underline{U}_h^k$,

$$\boxed{a_h(\underline{u}_h, \underline{v}_h) := a_{\nu,h}(\underline{u}_h, \underline{v}_h) + a_{\boldsymbol{\beta},\mu,h}(\underline{u}_h, \underline{v}_h) = l_h(\underline{v}_h)}$$

Discrete problem II

Lemma (Stability of a_h)

There is $\gamma_\varrho > 0$ independent of h, ν, $\boldsymbol{\beta}$ and μ s.t.

$$\forall \underline{w}_h \in \underline{U}_h^k, \qquad \|\underline{w}_h\|_{\sharp,h} \leqslant \gamma_\varrho \zeta^{-1} \sup_{\underline{v}_h \in \underline{U}_h^k \setminus \{0\}} \frac{a_h(\underline{w}_h, \underline{v}_h)}{\|\underline{v}_h\|_{\sharp,h}},$$

with $\zeta := \tau_{\mathrm{ref},T}\mu$ and stability norm

$$\|\underline{v}_h\|_{\sharp,h}^2 := \|\underline{v}_h\|_{\nu,h}^2 + \|\underline{v}_h\|_{\boldsymbol{\beta},\mu,h}^2 + \sum_{T \in \mathcal{T}_h} h_T \beta_{\mathrm{ref},T}^{-1} \|G_{\boldsymbol{\beta},T}^k \underline{v}_h\|_T^2$$

A modified reduction map

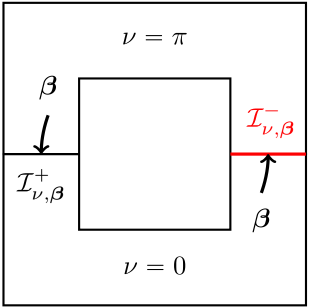

- Let $F \in \mathcal{F}_h^{\mathrm{i}}$ be such that $F \subset \mathcal{I}^{-}_{\nu,\boldsymbol{\beta}}$
- The trace of u is two-valued on F
- We interpolate the face unknown **from the diffusive side**

Convergence I

Theorem (Error estimate)

Assume that, for all $T \in \mathcal{T}_h$, $u \in H^{k+2}(T)$ and

$$h_T L_{\boldsymbol{\beta},T} \leqslant \beta_{\mathrm{ref},T} \quad \text{and} \quad h_T \mu \leqslant \beta_{\mathrm{ref},T},$$

Then, there is $C > 0$ independent of h, ν, $\boldsymbol{\beta}$, and μ s.t.

$$\|\underline{I}_h^k u - \underline{u}_h\|_{\sharp,h}^2 \leqslant C \sum_{T \in \mathcal{T}_h} \left\{ B_T^{\mathrm{d}}(u,k) h_T^{2(k+1)} + B_T^{\mathrm{a}}(u,k) \min(1, \mathrm{Pe}_T) h_T^{2(k+\frac{1}{2})} \right\},$$

with Pe_T denoting the local Péclet number.

Convergence II

- This estimate holds across the entire range for Pe_T
- In the diffusion-dominated regime $\mathrm{Pe}_T \leqslant h_T$, we have

$$\|\underline{I}_h^k u - \underline{u}_h\|_{\sharp,h} = \mathcal{O}(h^{k+1})$$

- In the advection-dominated regime $\mathrm{Pe}_T \geqslant 1$, we have

$$\|\underline{I}_h^k u - \underline{u}_h\|_{\sharp,h} = \mathcal{O}(h^{k+1/2})$$

- In between, we have intermediate orders of convergence

Numerical example I

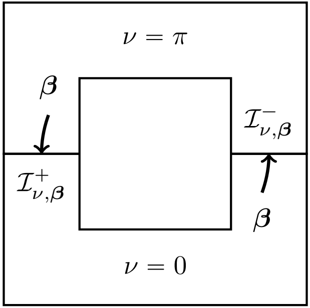

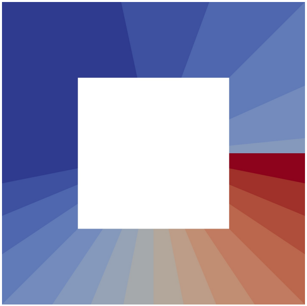

Figure: Two-dimensional example from [DP, Ern and Guermond, 2008]

Numerical example II

- Let $\Omega = (-1,1)^2 \backslash [-0.5, 0.5]^2$ and set

$$\nu(\theta, r) = \begin{cases} \pi & \text{if } 0 < \theta < \pi, \\ 0 & \text{if } \pi < \theta < 2\pi, \end{cases} \quad \boldsymbol{\beta}(\theta, r) = \frac{\boldsymbol{e}_\theta}{r}, \quad \mu = 1 \cdot 10^{-6}$$

- We consider the exact solution

$$u(\theta, r) = \begin{cases} (\theta - \pi)^2 & \text{if } 0 < \theta < \pi \\ 3\pi(\theta - \pi) & \text{if } \pi < \theta < 2\pi \end{cases}$$

Numerical example III

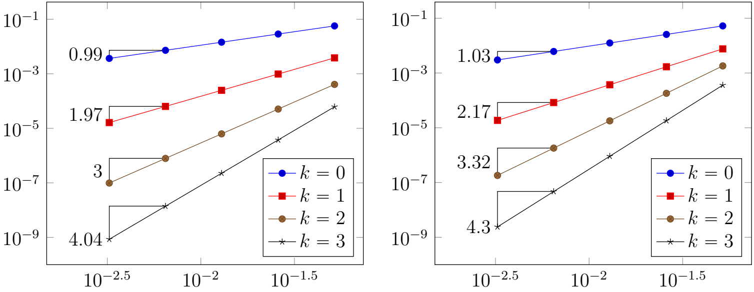

Figure: Energy (left) and L^2-norm (right) of the error vs. h

Outline

μBibliography: Linear elasticity

- On standard meshes
  - PEERS [Arnold, Brezzi and Douglas, 1984]
  - Nonconforming primal* $\mathbb{P}^1$ [Brenner and Sung, 1992]
  - Nonconforming mixed [Arnold and Winther, 2003]
  - Conforming mixed polynomial [Arnold and Winther, 2002]
  - Stabilized nonconforming primal [Hansbo and Larson, 2003]
- On polyhedral meshes
  - Conforming primal VE [Beirão da Veiga, Brezzi and Marini, 2013]
  - Generalized nonconforming $\mathbb{P}^1$ [DP and Lemaire, 2015]
  - Nonconforming primal HHO [DP and Ern, 2015]

Continuous setting

- Let $d \in \{2, 3\}$. We consider the problem: Find $\boldsymbol{u} : \Omega \to \mathbb{R}^d$ s.t.

$$\begin{aligned} -\boldsymbol{\nabla}\cdot\boldsymbol{\sigma}(\boldsymbol{u}) &= \boldsymbol{f} && \text{in } \Omega, \\ \boldsymbol{u} &= \boldsymbol{0} && \text{on } \partial\Omega \end{aligned}$$

  with real Lamé parameters $\lambda \geqslant 0$ and $\mu > 0$ and

$$\boldsymbol{\sigma}(\boldsymbol{u}) = 2\mu\boldsymbol{\nabla}_{\mathrm{s}}\boldsymbol{u} + \lambda(\boldsymbol{\nabla}\cdot\boldsymbol{u})\boldsymbol{I}_d$$

- $\lambda \to +\infty$ corresponds to quasi-incompressible materials
- More general BCs can be considered with minor modifications

Rigid body motions

- Applied to vector fields, the operator $\boldsymbol{\nabla}_{\mathrm{s}}$ yields strains
- Let $d = 3$. Its kernel $\mathrm{RM}(\Omega)$ contains rigid-body motions

$$\mathrm{RM}(\Omega) := \left\{ \boldsymbol{v} \in H^1(\Omega)^3 \mid \exists \boldsymbol{\alpha}, \boldsymbol{\omega} \in \mathbb{R}^3,\ \boldsymbol{v}(\boldsymbol{x}) = \boldsymbol{\alpha} + \boldsymbol{\omega} \otimes \boldsymbol{x} \right\}$$

- We note for further use that

$$\mathbb{P}_d^0(\Omega)^3 \subset \mathrm{RM}(\Omega) \subset \mathbb{P}_d^1(\Omega)^3$$

Features

- High-order method on general polyhedral meshes
- Locking-free primal formulation
- Global SPD system
- Strongly symmetric strain and stress tensors
- Low computational cost
  - In 3d, 9 DOFs/face for the lowest-order version $k = 1$
  - Compact stencil (face neighbours)
  - Simplified data exchange w.r. to vertex DOFs

DOFs and reduction map I

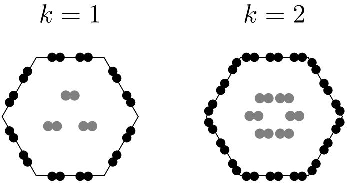

Figure: $\underline{\boldsymbol{U}}_T^k$ for $k \in \{1, 2\}$

- For $k \geqslant 1$ and all $T \in \mathcal{T}_h$, we define the local space of DOFs

$$\underline{\boldsymbol{U}}_T^k := \mathbb{P}_d^k(T)^d \times \left\{ \bigtimes_{F \in \mathcal{F}_T} \mathbb{P}_{d-1}^k(F)^d \right\}$$

- The global space has single-valued interface DOFs

$$\underline{\boldsymbol{U}}_h^k := \left\{ \bigtimes_{T \in \mathcal{T}_h} \mathbb{P}_d^k(T)^d \right\} \times \left\{ \bigtimes_{F \in \mathcal{F}_h} \mathbb{P}_{d-1}^k(F)^d \right\}$$

Displacement reconstruction I

- Let $T \in \mathcal{T}_h$. The local displacement reconstruction operator

$$\boldsymbol{p}_T^{k+1} : \underline{\boldsymbol{U}}_T^k \to \mathbb{P}_d^{k+1}(T)^d$$

is s.t., for all $\underline{\boldsymbol{v}}_T = \big(\boldsymbol{v}_T, (\boldsymbol{v}_F)_{F\in\mathcal{F}_T}\big) \in \underline{\boldsymbol{U}}_T^k$ and $\boldsymbol{w} \in \mathbb{P}_d^{k+1}(T)^d$,

$$\boxed{(\boldsymbol{\nabla}_{\rm s}\boldsymbol{p}_T^{k+1}\underline{\boldsymbol{v}}_T, \boldsymbol{\nabla}_{\rm s}\boldsymbol{w})_T = -(\boldsymbol{v}_T, \boldsymbol{\nabla}{\cdot}\boldsymbol{\nabla}_{\rm s}\boldsymbol{w})_T + \sum_{F\in\mathcal{F}_T}(\boldsymbol{v}_F, \boldsymbol{\nabla}_{\rm s}\boldsymbol{w}\boldsymbol{n}_{TF})_F}$$

- Rigid-body motions are prescribed from $\underline{\boldsymbol{v}}_T$ setting

$$\int_T \boldsymbol{p}_T^{k+1}\underline{\boldsymbol{v}}_T = \int_T \boldsymbol{v}_T, \quad \int_T \boldsymbol{\nabla}_{\rm ss}\boldsymbol{p}_T^{k+1}\underline{\boldsymbol{v}}_T = \sum_{F\in\mathcal{F}_T}\int_F \frac{1}{2}(\boldsymbol{n}_{TF}\otimes\boldsymbol{v}_F - \boldsymbol{v}_F\otimes\boldsymbol{n}_{TF})$$

Displacement reconstruction II

Lemma (Approximation properties for $\boldsymbol{p}_T^{k+1}\underline{\boldsymbol{I}}_T^k$)

There exists $C > 0$ independent of h_T s.t., for all $\boldsymbol{v} \in H^{k+2}(T)^d$,

$$\|\boldsymbol{v} - \boldsymbol{p}_T^{k+1}\underline{\boldsymbol{I}}_T^k\boldsymbol{v}\|_T + h_T\|\boldsymbol{\nabla}(\boldsymbol{v} - \boldsymbol{p}_T^{k+1}\underline{\boldsymbol{I}}_T^k\boldsymbol{v})\|_T \leqslant Ch_T^{k+2}\|\boldsymbol{v}\|_{H^{k+2}(T)^d}.$$

Proceeding as for Poisson, one can prove the Euler equation

$$(\boldsymbol{\nabla}_{\rm s}\boldsymbol{p}_T^{k+1}\underline{\boldsymbol{I}}_T^k\boldsymbol{v} - \boldsymbol{\nabla}_{\rm s}\boldsymbol{v}, \boldsymbol{\nabla}_{\rm s}\boldsymbol{w})_T = 0 \qquad \forall \boldsymbol{w} \in \mathbb{P}_d^{k+1}(T)^d,$$

and the approximation properties follow.

Stabilization I

- Define, for $T \in \mathcal{T}_h$, the stabilization bilinear form s_T as

$$s_T(\underline{\boldsymbol{u}}_T, \underline{\boldsymbol{v}}_T) := \sum_{F \in \mathcal{F}_T} h_F^{-1} (\pi_F^k(\widehat{\boldsymbol{p}}_T^{k+1} \underline{\boldsymbol{u}}_T - \boldsymbol{u}_F), \pi_F^k(\widehat{\boldsymbol{p}}_T^{k+1} \underline{\boldsymbol{v}}_T - \boldsymbol{v}_F))_F,$$

  with displacement reconstruction $\widehat{\boldsymbol{p}}_T^{k+1} : \underline{\boldsymbol{U}}_T^k \to \mathbb{P}_d^{k+1}(T)^d$ s.t.

$$\widehat{\boldsymbol{p}}_T^{k+1} \underline{\boldsymbol{v}}_T := \boldsymbol{v}_T + (\boldsymbol{p}_T^{k+1} \underline{\boldsymbol{v}}_T - \pi_T^k \boldsymbol{p}_T^{k+1} \underline{\boldsymbol{v}}_T)$$

- We express stability w.r. to the discrete strain norm

$$\|\underline{\boldsymbol{v}}_T\|_{\varepsilon,T}^2 := \|\boldsymbol{\nabla}_{\mathrm{s}} \boldsymbol{v}_T\|_T^2 + \sum_{F \in \mathcal{F}_T} h_F^{-1} \|\boldsymbol{v}_F\|_F^2$$

Stabilization II

Lemma (Stability and approximation)

Let $T \in \mathcal{T}_h$ and assume $k \geqslant 1$. Then,

$$\|\underline{\boldsymbol{v}}_T\|_{\varepsilon,T}^2 \lesssim \|\boldsymbol{\nabla}_{\rm s}\boldsymbol{p}_T^{k+1}\underline{\boldsymbol{v}}_T\|_T^2 + s_T(\underline{\boldsymbol{v}}_T, \underline{\boldsymbol{v}}_T) \lesssim \|\underline{\boldsymbol{v}}_T\|_{\varepsilon,T}^2.$$

Moreover, for all $\boldsymbol{v} \in H^{k+2}(T)^d$, we have

$$\left\{\|\boldsymbol{\nabla}_{\rm s}(\boldsymbol{p}_T^{k+1}\underline{\boldsymbol{I}}_T^k\boldsymbol{v} - \boldsymbol{v})\|_T^2 + s_T(\underline{\boldsymbol{I}}_T^k\boldsymbol{v}, \underline{\boldsymbol{I}}_T^k\boldsymbol{v})\right\}^{1/2} \lesssim h_T^{k+1}\|\boldsymbol{v}\|_{H^{k+2}(T)^d}.$$

Classical result for $k = 0$: Crouzeix–Raviart does not meet Korn!

Stabilization III

- For all $F \in \mathcal{F}_T$ one has, inserting $\pm\pi_F^k \widehat{\boldsymbol{p}}_T^{k+1} \underline{\boldsymbol{v}}_T$,

$$\|\boldsymbol{v}_F - \boldsymbol{v}_T\|_F \lesssim \|\pi_F^k(\boldsymbol{v}_F - \widehat{\boldsymbol{p}}_T^{k+1}\underline{\boldsymbol{v}}_T)\|_F + h_F^{-1/2}\|\boldsymbol{p}_T^{k+1}\underline{\boldsymbol{v}}_T - \pi_T^k \boldsymbol{p}_T^{k+1}\underline{\boldsymbol{v}}_T\|_T$$

- For any function $\boldsymbol{w} \in H^1(T)^d$ with rigid-body motions $\boldsymbol{w}_{\mathrm{RM}}$,

$$\|\boldsymbol{w} - \pi_T^k \boldsymbol{w}\|_T = \|(\boldsymbol{w} - \boldsymbol{w}_{\mathrm{RM}}) - \pi_T^k(\boldsymbol{w} - \boldsymbol{w}_{\mathrm{RM}})\|_T \lesssim h_T \|\boldsymbol{\nabla}_{\mathrm{s}} \boldsymbol{w}\|_T$$

  where $\pi_T^k \boldsymbol{w}_{\mathrm{RM}} = \boldsymbol{w}_{\mathrm{RM}}$ requires $k \geqslant 1$ to have

$$\mathrm{RM}(T) \subset \mathbb{P}_d^k(T)^d$$

- Clearly, this reasoning breaks down for $k = 0$

Divergence reconstruction

- We define the local local discrete divergence operator

$$D_T^k : \underline{\boldsymbol{U}}_T^k \to \mathbb{P}_d^k(T)$$

s.t., for all $\underline{\boldsymbol{v}}_T = \big(\boldsymbol{v}_T, (\boldsymbol{v}_F)_{F \in \mathcal{F}_T}\big) \in \underline{\boldsymbol{U}}_T^k$ and all $q \in \mathbb{P}_d^k(T)$,

$$\boxed{(D_T^k \underline{\boldsymbol{v}}_T, q)_T := -(\boldsymbol{v}_T, \boldsymbol{\nabla} q)_T + \sum_{F \in \mathcal{F}_T} (\boldsymbol{v}_F \cdot \boldsymbol{n}_{TF}, q)_F}$$

- By construction, we have the following commuting diagram:

$$\begin{array}{ccc} \boldsymbol{H}^1(T) & \xrightarrow{\boldsymbol{\nabla}\cdot} & L^2(T) \\ \Big\downarrow \underline{\boldsymbol{I}}_T^k & & \Big\downarrow \pi_T^k \\ \underline{\boldsymbol{U}}_T^k & \xrightarrow{D_T^k} & \mathbb{P}_d^k(T) \end{array}$$

Discrete problem

- We define the local bilinear form a_T on $\underline{\boldsymbol{U}}_T^k \times \underline{\boldsymbol{U}}_T^k$ as

$$a_T(\underline{\boldsymbol{u}}_T, \underline{\boldsymbol{v}}_T) := 2\mu(\boldsymbol{\nabla}_{\rm s}\boldsymbol{p}_T^{k+1}\underline{\boldsymbol{u}}_T, \boldsymbol{\nabla}_{\rm s}\boldsymbol{p}_T^{k+1}\underline{\boldsymbol{v}}_T)_T \\ + \lambda(D_T^k\underline{\boldsymbol{u}}_T, D_T^k\underline{\boldsymbol{v}}_T) + (2\mu)s_T(\underline{\boldsymbol{u}}_T, \underline{\boldsymbol{v}}_T)$$

- The discrete problem reads: Find $\underline{\boldsymbol{u}}_h \in \underline{\boldsymbol{U}}_{h,0}^k$ s.t.

$$\boxed{a_h(\underline{\boldsymbol{u}}_h, \underline{\boldsymbol{v}}_h) := \sum_{T\in\mathcal{T}_h} a_T(\underline{\boldsymbol{u}}_T, \underline{\boldsymbol{v}}_T) = \sum_{T\in\mathcal{T}_h} (\boldsymbol{f}, \boldsymbol{v}_T)_T \quad \forall \underline{\boldsymbol{v}}_h \in \underline{\boldsymbol{U}}_{h,0}^k}$$

with $\underline{\boldsymbol{U}}_{h,0}^k$ incorporating boundary conditions

Convergence I

Theorem (Energy-norm error estimate)

Assume $k \geqslant 1$ *and the additional regularity*

$$\boldsymbol{u} \in H^{k+2}(\Omega)^d \text{ and } \boldsymbol{\nabla}\cdot\boldsymbol{u} \in H^{k+1}(\Omega).$$

Then, there exists $C > 0$ *independent of* h, μ, *and* λ *s.t.*

$$(2\mu)^{1/2}\|\underline{\boldsymbol{u}}_h - \widehat{\underline{\boldsymbol{u}}}_h\|_{a,h} \leqslant Ch^{k+1}B(\boldsymbol{u},k),$$

with

$$B(\boldsymbol{u},k) := (2\mu)\|\boldsymbol{u}\|_{H^{k+2}(\Omega)^d} + \lambda\|\boldsymbol{\nabla}\cdot\boldsymbol{u}\|_{H^{k+1}(\Omega)}.$$

Convergence II

- Locking-free if $B(\boldsymbol{u}, k)$ is bounded uniformly in λ
- For $d = 2$ and Ω convex, one has using Cattabriga's regularity

$$B(\boldsymbol{u}, 0) = \|\boldsymbol{u}\|_{H^2(\Omega)^d} + \lambda \|\boldsymbol{\nabla}\cdot\boldsymbol{u}\|_{H^1(\Omega)} \leqslant C_\mu \|\boldsymbol{f}\|$$

- More generally, for $k \geqslant 1$, we need the regularity shift

$$\boxed{B(\boldsymbol{u}, k) \leqslant C_\mu \|\boldsymbol{f}\|_{H^k(\Omega)^d}}$$

- **Key point: commuting property for D_T^k**

Convergence III

Theorem (L^2-error estimate for the displacement)

Assuming elliptic regularity for Ω and provided that

$$\boldsymbol{u} \in H^{k+2}(\Omega)^d \text{ and } \boldsymbol{\nabla}\cdot\boldsymbol{u} \in H^{k+1}(\Omega),$$

it holds with $C>0$ independent of λ and h,

$$\|\boldsymbol{u}_h - \pi_h^k \boldsymbol{u}\| \leqslant C h^{k+2} B(\boldsymbol{u}, k),$$

with $\boldsymbol{u}_h$ s.t. $\boldsymbol{u}_{h|T} = \boldsymbol{u}_T$ for all $T \in \mathcal{T}_h$.

Numerical example I

- We consider the following exact solution:

$$\boldsymbol{u}(\boldsymbol{x}) = \big(\sin(\pi x_1)\sin(\pi x_2) + (2\lambda)^{-1}x_1, \cos(\pi x_1)\cos(\pi x_2) + (2\lambda)^{-1}x_2\big)$$

- The solution u has vanishing divergence in the limit $\lambda \to +\infty$:

$$\boldsymbol{\nabla}\cdot\boldsymbol{u}(\boldsymbol{x}) = \frac{1}{\lambda}$$

Numerical example II

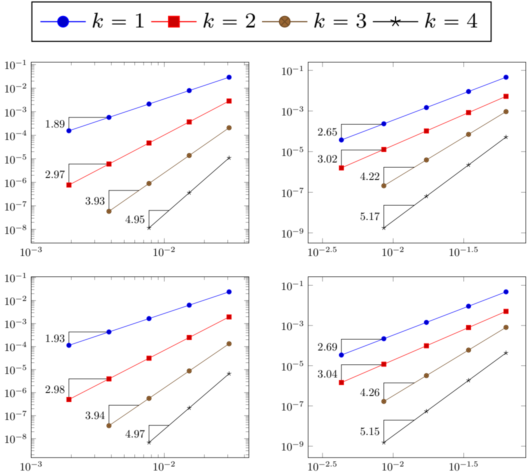

Figure: Energy error with $\lambda = 1$ (above) and $\lambda = 1000$ (below) vs. h for the triangular (left) and hexagonal (right) mesh families

Numerical example III

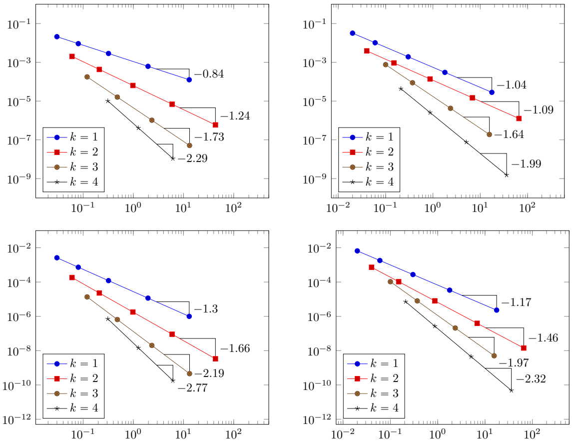

Figure: Energy (above) and displacement (below) error vs. τ_{tot} (s) for the triangular and hexagonal mesh families

Numerical example IV

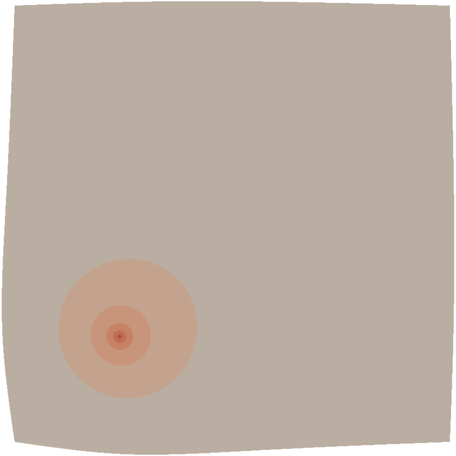

Figure: HHO + dG applied to poro-elasticity, [Boffi et al., 2015]

References I

Antonietti, P. F., Giani, S., and Houston, P. (2013).
hp-version composite discontinuous Galerkin methods for elliptic problems on complicated domains.
SIAM J. Sci. Comput, 35(3):A1417–A1439.

Arnold, D. N., Brezzi, F., Cockburn, B., and Marini, L. D. (2002).
Unified analysis of discontinuous Galerkin methods for elliptic problems.
SIAM J. Numer. Anal., 39(5):1749–1779.

Arnold, D. N., Brezzi, F., and Douglas, J. (1984).
PEERS: A new mixed finite element for plane elasticity.
Japan Journal of Industrial and Applied Mathematics, 1(2):347–367.

Arnold, D. N. and Winther, R. (2002).
Mixed finite elements for elasticity.
Numer. Math., 92(3):401–419.

Arnold, D. N. and Winther, R. (2003).
Nonconforming mixed elements for elasticity.
Math. Models Methods Appl. Sci., 13(3):295–307.
Dedicated to Jim Douglas, Jr. on the occasion of his 75th birthday.

Ayuso de Dios, B., Lipnikov, K., and Manzini, G. (2014).
The nonconforming virtual element method.
Submitted. ArXiV preprint arXiv:1405.3741.

Bassi, F., Botti, L., Colombo, A., Di Pietro, D. A., and Tesini, P. (2012).
On the flexibility of agglomeration based physical space discontinuous Galerkin discretizations.
J. Comput. Phys., 231(1):45–65.

Beirão da Veiga, L., Brezzi, F., Cangiani, A., Manzini, G., Marini, L. D., and Russo, A. (2013a).
Basic principles of virtual element methods.
Math. Models Methods Appl. Sci., 23:199–214.

References II

Beirão da Veiga, L., Brezzi, F., and Marini, L. (2013b).
Virtual elements for linear elasticity problems.
SIAM J. Numer. Anal., 51(2):794–812.

Boffi, D., Botti, M., and Di Pietro, D. A. (2015).
A nonconforming high-order method for the Biot problem on general meshes.
Submitted. Preprint arXiv:1506.03722.

Bonelle, J. and Ern, A. (2014).
Analysis of compatible discrete operator schemes for elliptic problems on polyhedral meshes.
M2AN Math. Model. Numer. Anal., 48:553–581.

Brenner, S. C. and Sung, L.-Y. (1992).
Linear finite element methods for planar linear elasticity.
Math. Comp., 59(200):321–338.

Brezzi, F., Lipnikov, K., and Shashkov, M. (2005).
Convergence of the mimetic finite difference method for diffusion problems on polyhedral meshes.
SIAM J. Numer. Anal., 43(5):1872–1896.

Cockburn, B., Di Pietro, D. A., and Ern, A. (2015).
Bridging the Hybrid High-Order and Hybridizable Discontinuous Galerkin methods.
Submitted. Preprint hal-01115318.

Cockburn, B., Gopalakrishnan, J., and Lazarov, R. (2009).
Unified hybridization of discontinuous Galerkin, mixed, and continuous Galerkin methods for second order elliptic problems.
SIAM J. Numer. Anal., 47(2):1319–1365.

Di Pietro, D. A. (2012).
Cell centered Galerkin methods for diffusive problems.
M2AN Math. Model. Numer. Anal., 46(1):111–144.

References III

Di Pietro, D. A., Droniou, J., and Ern, A. (2014a).
A discontinuous-skeletal method for advection-diffusion-reaction on general meshes.
Preprint arXiv:1411.0098.

Di Pietro, D. A. and Ern, A. (2012).
Mathematical aspects of discontinuous Galerkin methods, volume 69 of *Mathématiques & Applications*.
Springer-Verlag, Berlin.

Di Pietro, D. A. and Ern, A. (2015).
A hybrid high-order locking-free method for linear elasticity on general meshes.
Comput. Methods Appl. Mech. Engrg., 283:1–21.
DOI: 10.1016/j.cma.2014.09.009.

Di Pietro, D. A., Ern, A., and Guermond, J.-L. (2008).
Discontinuous Galerkin methods for anisotropic semi-definite diffusion with advection.
SIAM J. Numer. Anal., 46(2):805–831.

Di Pietro, D. A., Ern, A., and Lemaire, S. (2014b).
An arbitrary-order and compact-stencil discretization of diffusion on general meshes based on local reconstruction operators.
Comput. Methods Appl. Math., 14(4):461–472.
DOI: 10.1515/cmam-2014-0018.

Di Pietro, D. A. and Lemaire, S. (2015).
An extension of the Crouzeix–Raviart space to general meshes with application to quasi-incompressible linear elasticity and Stokes flow.
Math. Comp., 84(291):1–31.

Droniou, J. and Eymard, R. (2006).
A mixed finite volume scheme for anisotropic diffusion problems on any grid.
Numer. Math., 105:35–71.

References IV

Droniou, J., Eymard, R., Gallouët, T., and Herbin, R. (2010).
A unified approach to mimetic finite difference, hybrid finite volume and mixed finite volume methods.
M3AS Mathematical Models and Methods in Applied Sciences, 20(2):1–31.

Eymard, R., Gallouët, T., and Herbin, R. (2010).
Discretization of heterogeneous and anisotropic diffusion problems on general nonconforming meshes. SUSHI: a scheme using stabilization and hybrid interfaces.
IMA J. Numer. Anal., 30(4):1009–1043.

Eymard, R., Henry, G., Herbin, R., Hubert, F., Klöfkorn, R., and Manzini, G. (2011).
3D benchmark on discretization schemes for anisotropic diffusion problems on general grids.
In *Finite Volumes for Complex Applications VI - Problems & Perspectives*, volume 2, pages 95–130. Springer.

Gastaldi, F. and Quarteroni, A. (1989).
On the coupling of hyperbolic and parabolic systems: Analytical and numerical approach.
Appl. Numer. Math., 6:3–31.

Hansbo, P. and Larson, M. G. (2003).
Discontinuous Galerkin and the Crouzeix–Raviart element: application to elasticity.
M2AN Math. Model. Numer. Anal., 37(1):63–72.

Herbin, R. and Hubert, F. (2008).
Benchmark on discretization schemes for anisotropic diffusion problems on general grids.
In Eymard, R. and Hérard, J.-M., editors, *Finite Volumes for Complex Applications V*, pages 659–692. John Wiley & Sons.

Kuznetsov, Y., Lipnikov, K., and Shashkov, M. (2004).
Mimetic finite difference method on polygonal meshes for diffusion-type problems.
Comput. Geosci., 8:301–324.

Wang, J. and Ye, X. (2013).
A weak Galerkin element method for second-order elliptic problems.
J. Comput. Appl. Math., 241:103–115.